Ginkgo leaf cuticle chemistry across changing pCO_2 regimes

Phillip E. Jardine[1], Matthew Kent[2], Wesley T. Fraser[3], and Barry H. Lomax[2]

[1]Institute of Geology and Palaeontology, University of Münster, 48149 Münster, Germany. jardine@uni-muenster.de

[2]Agriculture and Environmental Science, University of Nottingham, Sutton Bonington Campus, Leicestershire, LE12 5RD, UK. Matthew.Kent@nottingham.ac.uk, Barry.Lomax@nottingham.ac.uk

[3]Geography, Department of Social Sciences, Oxford Brookes University, Oxford OX3 0BP, UK. wfraser@brookes.ac.uk

Abstract

Cuticles have been a key part of palaeobotanical research since the mid-19th Century. Recently, cuticular research has moved beyond morphological traits to incorporate the chemical signature of modern and fossil cuticles, with the aim of using this as a taxonomic and classification tool. For this approach to work, cuticle chemistry would have to maintain a strong taxonomic signal, with a limited input from the ambient environment in which the plant grew. Here, we use attenuated total reflectance Fourier Transform infrared (ATR-FTIR) spectroscopy to analyse leaf cuticles from *Ginkgo biloba* plants grown in experimentally enhanced CO_2 conditions, to test for the impact of changing CO_2 regimes on cuticle chemistry. We find limited evidence for an impact of CO_2 on the chemical signature of *Ginkgo* cuticles, with more pronounced differences demonstrated between the abaxial (lower leaf surface) and adaxial (upper leaf surface) cuticles. These findings support the use of chemotaxonomy for plant cuticular remains across geological timescales, and the concomitant large-scale variations in CO_2 concentrations.

Keywords cuticle, *Ginkgo*, CO_2, ATR-FTIR, chemotaxonomy, geochemistry

Introduction

The plant cuticle is a key evolutionary innovation that enabled plants to colonise subaerial environments in the early Palaeozoic (Domínguez et al. 2011; Renault et al. 2017; Salminen et al. 2018). It is a waxy and waterproof membrane that covers the outer surface of the green parts of plants, preventing desiccation and providing structural support, as well as protection from ultraviolet (UV) irradiance, herbivory, and infection (Kerp 1990; Domínguez et al. 2011; Heredia-Guerrero et al. 2014; Dominguez et al. 2017). Cuticles consist of an insoluble aliphatic matrix comprising cutin (a long chain polymer composed of esterified fatty acids), cutan (an ether-linked hydrocarbon polymer), or a mixture of the two. Distributed through the matrix are soluble waxes and phenolic compounds; waxes also occur on the outer surface of the matrix. The inner part of the matrix, which connects with the epidermal cells, contains a high concentration of polysaccharides (Domínguez et al. 2011; Heredia-Guerrero et al. 2014; Dominguez et al. 2017).

Plant cuticles have been investigated and utilised by palaeobotanists for over 170 years (Kerp 1990). Cuticles have a high preservation potential, retaining anatomical details such as epidermal cell morphologies and stomata distributions (Kerp 1990), and have therefore been used in a variety of applications, including fossil plant taxonomy and determining the botanical affinities of disparate plant organs (Kerp 1990; Kerp et al. 2006; Abu Hamad et al. 2008; Bomfleur et al. 2013; Abu Hamad et al. 2017), reconstructing atmospheric *p*CO2 from stomatal densities or associated indices (Woodward 1987; McElwain and Chaloner 1995; Lomax and Fraser 2015; McElwain and Steinthorsdottir 2017; Steinhorsdottir et al. 2018), and reconstructing genome size based on guard cell length (Lomax et al. 2014). Recently, Steinthorsdottir et al. (2018) suggested that morphological

changes in the cuticle surface, such as stomatal complex distortion and disorganised cell arrangements, could be a potential proxy for volcanic SO_2 emissions.

In addition to morphology-based analyses of cuticles, other studies have focused on utilising cuticle chemistry. One area of interest has been generating carbon isotope data from dispersed cuticles and thereby reconstructing carbon cycle dynamics (e.g. Peters-Kottig et al. 2006; Richey et al. 2018), and by combining with isotopic estimates of the $\delta^{13}C$ of the atmosphere it may be possible to determine changes in water use efficiency (Diefendorf et al. 2010). Molecular analysis (e.g. by pyrolysis-gas chromatography-mass spectrometry) of cuticle has also provided a wealth of information, including the chemical composition of cuticles, the distribution of cutin and cutan among plant taxa, and the fate of these biopolymers in the geological record (Tegelaar et al. 1993; Mösle et al. 1997; Mösle et al. 1998; Collinson et al. 1999; Zodrow and Mastalerz 2001; Mösle et al. 2002; Zodrow and Mastalerz 2002; Gupta et al. 2007a; Gupta et al. 2007b; Zodrow et al. 2012a; Zodrow et al. 2012b; see also Gupta 2014 for review).

Vibrational spectroscopic techniques such as Fourier transform infrared (FTIR) and Raman spectroscopy have also been used to analyse cuticle chemistry, because they have the advantages of being non-destructive, efficient and able to analyse very small sample quantities (Heredia-Guerrero et al. 2014; Olcott Marshall and Marshall 2014). These approaches have been employed in both modern and fossil settings, with the aims of understanding cuticle chemistry and its response to environmental change and ontogenetic development (Villena et al. 2000; Ribeiro da Luz 2006; Dominguez et al. 2012; Littlejohn et al. 2015; Innes et al. 2019; Liu et al. 2019), diagenesis/fossilisation processes and the characterisation of organic matter in the geological record (Lyons et al. 1995; Collinson et al.

1999; Zodrow et al. 2000; Zodrow and Mastalerz 2002; D'Angelo 2006; Zodrow et al. 2009; Zodrow and Mastalerz 2009; D'Angelo et al. 2010; D'Angelo et al. 2011; Zodrow et al. 2012a; Zodrow et al. 2012b; D'Angelo and Zodrow 2015; Zodrow et al. 2016), and the taxonomic identification of plants using their chemical signature (termed chemotaxonomy) (Zodrow and Mastalerz 2001, 2002; D'Angelo 2006; D'Angelo et al. 2010; D'Angelo and Zodrow 2015; Vajda et al. 2017). Cuticle chemistry has been shown to contain a phylogenetic signal that is preserved in fossil material, leading to the possibility of classifying fragmentary or otherwise problematic cuticular remains (Vajda et al. 2017). Parallel developments have been made in pollen and spore research (Pappas et al. 2003; Dell'Anna et al. 2009; Steemans et al. 2010; Zimmermann and Kohler 2014; Julier et al. 2016; Zimmermann et al. 2016), suggesting that FTIR or Raman based chemotaxonomy may have much to offer for palaeobotanical and palynological investigations.

For cuticle chemistry to be successfully used for chemotaxonomy, it is critical to understand the other possible controls on the chemical signature that may bias or obscure any taxonomic or phylogenetic signal. Changing ambient UV-B levels are expected to drive variations in the concentrations of phenolic compounds, for example, since these form the UV-B absorbing compounds (UACs) in the plant cuticle (Blokker et al. 2006; Rozema et al. 2009). Such a relationship has been demonstrated in *Polylepis tarapacana* in the Bolivian Andes (Gonzalez et al. 2007) and *Fagus sylvatica* from the Hunsrück region of Germany (Neitzke and Therburg 2003), where leaf UAC concentrations increased with increased UV-B at higher altitudes (although it should be noted that these findings relate to bulk leaf tissue, rather than isolated cuticles). Over longer geological timescales, atmospheric CO_2 concentration may be a more important parameter, because it has varied from ~200 to ~2000 ppm since the appearance of the earliest plant cuticles >400 Ma (McElwain and

105 Steinthorsdottir 2017) (Fig. 1); however, the impacts of changes in atmospheric CO_2
106 concentrations on cuticle chemistry are currently not well understood. From a carbon
107 economic perspective, in a high CO_2 world such as the early Mesozoic biomolecules with a
108 high carbon content and thus metabolite cost would be cheaper to construct due to an increase
109 in substrate, suggesting a response to changes in CO_2 is expected. While a strong cuticular
110 chemical response to CO_2 would possibly limit the use of chemotaxomony across long
111 timescales, it could open up the possibility of new indicators of palaeo-CO_2 concentrations.
112
113 Here we investigate the effect of different CO_2 regimes on *Ginkgo biloba* leaf cuticle
114 chemistry. *Ginkgo* is a particularly relevant taxon for addressing this uncertainty because of
115 its longevity: *Ginkgo* first appeared in the early Mesozoic, and Ginkgoales in the late
116 Palaeozoic (Zhiyan and Xiangwu 2006), and this group has therefore existed across a wide
117 range of CO_2 regimes (Fig. 1). Modern and fossil *Ginkgo* cuticles have also been the subject
118 of past chemical research, meaning that the overall chemistry and diagenetic changes are
119 broadly understood (Mösle et al. 1997, 1998; Collinson et al. 1999).
120
121 **Methods**
122 The leaf cuticles analysed in this study were taken from *Ginkgo biloba* plants
123 experimentally grown under elevated CO_2 conditions, the full details of which can be found
124 in Gill et al. (2018). Briefly, *Ginkgo biloba* seedlings were grown for 6 months in walk-in
125 growth room chambers (UNIGRO, UK) at CO_2 concentrations of 400, 1200 and 2000 ppm.
126 Levington M3 was used as a potting medium, and the plants were kept well-watered during
127 the growth period. The plants were grown in a simulated day/night program with 10 hours of
128 light (300 µmol/m^2/s) per day, a night high temperature of 17°C and a daytime peak
129 temperature of 22°C. Relative humidity was held at 70%. After 6 months, leaves were

harvested from the plants and dried at 60°C. For our FTIR analyses we generated data for 2 plants per CO_2 treatment, using pre-cut leaf discs from 3 leaves per plant, resulting in a total of 18 leaves analysed.

IR spectra were generated using a Cary 670 FTIR spectrometer integrated with a Cary 620 FTIR microscope (Agilent, Santa Clara, CA, USA). The FTIR microscope was fitted with a 64x64 pixel focal plane array (FPA) detector, and a 15x Vis/IR objective at high magnification to which a Germanium crystal micro-attenuated total reflectance (ATR) was fitted, achieving a resolution of 1.1 µm per pixel (each pixel results in one IR spectrum, so that each measurement yields an array of 64 x 64 = 4096 spectra). Three replicate measurements per leaf disc (abaxial side) were collected at 64 scans per measurement and a resolution of 8, except for one of the 2000 ppm leaf discs where only two high quality measurements were obtained. Background spectra were collected prior to each set of replicates and automatically removed from the sample spectra. While we focused on the abaxial surface, the adaxial surface from one leaf disc per CO_2 treatment was also analysed, again with three replicate measurements, to compare chemical signals between the leaf sides.

The Cary 620 FTIR microscope allows a live view of the FPA detector which maximises the potential of good contact between the ATR crystal and the sample. At a micro-scale, the leaf surface was irregular and contact between the ATR Germanium crystal and the leaf was not uniform, resulting in variable quality of spectra across the measurement array. For each measurement, spectra were therefore extracted from those pixels where the height (=absorbance value) of the 1167 cm^{-1} peak exceeded 15% of the maximum 1167 cm^{-1} peak height within the array. The 1167 cm^{-1} peak was chosen because it is clearly present in all spectra (Figs. 2 and 3), and 15% of the maximum peak height was used as a threshold

because it provides a reasonable trade-off between obtaining high quality spectra and incorporating a sufficient number of spectra in each measurement. The mean of the extracted spectra was then calculated to provide one spectrum per replicate measurement.

Some spectra showed strong distortion in the higher wavenumbers, and so all were limited to <3100 cm^{-1} prior to analysis. Baseline curvature was removed with a 4^{th} order polynomial baseline, and the corrected spectra *z*-score standardised (i.e. the mean was subtracted and the spectra divided by the standard deviation, resulting with each spectrum having a mean of zero and a standard deviation of one). Peak assignment was carried out with reference to the published literature (Ramirez et al. 1992; Heredia-Guerrero et al. 2014).

Spectral changes across the CO_2 treatments were analysed in two ways: with Principal Components Analysis (PCA) and by measuring the heights of selected peaks. PCA is an exploratory multivariate technique that partitions data into axes of maximal variation (principal components), allowing complex multivariate data to be viewed in a limited number of dimensions. Some spectra showed distortion in the 2800 to 1800 cm^{-1} range, even after the 4^{th} order polynomial baseline correction, and this was found to swamp the PCA analysis such that it dominated the first axis (the principal component that explains most variation in the data). Prior to PCA the raw spectra were therefore limited to <1800 cm^{-1}, baseline corrected with a linear baseline, and *z*-score transformed. We ran the PCA on leaf disc mean spectra rather than on the individual replicates, to help bring out any major differences among CO_2 treatments and leaf surfaces (abaxial versus adaxial), as opposed to random among-replicate variation. Processing the spectra with Savitzky-Golay smoothing and taking derivatives did not substantially alter the distribution of samples in ordination space, so we focused our

179 analyses on the unprocessed spectra to make interpretation of loadings plots more
180 straightforward.
181
182 Peak height measurements were similar when taken from both the <3100 cm^{-1} spectra
183 with a 4^{th} order polynomial baseline correction and <1800 cm^{-1} spectra with a linear baseline
184 correction. We therefore used the <3100 cm^{-1} spectra, so as to include the aliphatic peaks at
185 2920 and 2850 cm^{-1}. Peaks were selected so that changes across the different components of
186 the cuticle (i.e. cutin, waxes, phenolic compounds, and polysaccharides; previous research
187 has shown that *Ginkgo* cuticles contain no cutan (Mösle et al. 1997)) could be detected, and
188 peak height was measured as the maximum absorbance value within a predetermined range
189 (see Table 1 for details). All data analysis was carried out in R v.3.4.2 (R Core Team 2017)
190 using the packages baseline v.1.2-1 (Liland and Mevik 2015) and prospectr v.0.1.3 (Stevens
191 and Ramirez-Lopez 2013). IR spectral data are provided in the supplementary information.
192
193 **Results**
194 ATR-FTIR spectra of the *Gingko* cuticles reveals many of the same peaks that have
195 been previously identified in other studies (Fig. 2). Specifically, peaks relating to aliphatic
196 compounds in cutin and waxes are located at 2920 cm^{-1} (CH_2 asymmetric stretching), 2850
197 cm^{-1} (CH_2 symmetric stretching), 1460 cm^{-1} and 1370 cm^{-1} (both CH_2 bending), peaks related
198 to ester vibrations in cutin are located at 1710 cm^{-1} (with shoulders at 1730 cm^{-1} and 1685
199 cm^{-1}; C=O stretching), 1167 cm^{-1} and 1104 cm^{-1} (both C-O-C stretching), peaks related to
200 phenolic compounds are located at 1605 cm^{-1} (C-C stretching) and 1515 cm^{-1} (C-C stretching
201 conjugated with C=C), and peaks related to polysaccharides are located at 1245 cm^{-1} (OH
202 bending; this peak may also represent cutin) and 1020 cm^{-1} (C-O stretching). Most of the
203 same peaks are present in both the abaxial and adaxial cuticles, although the abaxial cuticles

have a relatively higher 1167 cm^{-1} ester peak and 1605 cm^{-1} aromatic peak, related to cutin and phenolic compounds, respectively, and the adaxial cuticles have a pronounced 1720 cm^{-1} ester peak and a relatively higher 1245 cm^{-1} hydroxyl peak, related to cutin and polysaccharides or cutin, respectively (Fig. 3). The spectra do not show any obvious differences across CO_2 treatments (Fig. 3).

A PCA of the spectral data shows the major variability in the dataset is partitioned between the abaxial and adaxial cuticles, which are separated on axis 1 of the ordination, and to some extent on axis 4 (Fig. 4). There are no clear groupings associated with CO_2 treatment on any of the first four PCA axes, which together account for >90% of the variation in the data. Loadings plots show that PCA axis 1 is driven by variations in the 1720 and 1245 cm^{-1} peaks (positive relationship; these peaks are higher in the adaxial cuticles) and peaks between 1000 and 1100 cm^{-1} (negative relationship). Axes 2 and 3 are primarily driven by variations around 1700 cm^{-1}, while the distribution of samples on axis 4 is underpinned by variations in the height of the 1167 cm^{-1} peak, which again differs between the abaxial and adaxial cuticles. This lack of a chemical change with increasing CO_2 is also shown in the 2^{nd} derivative of Savitzky-Golay smoothed spectra, and when only the abaxial cuticles are ordinated (Fig. S1).

Analysis of peak heights suggests that there are limited consistent changes with CO_2 level (Fig. 5). One possible exception is the 1460 cm^{-1} aliphatic peak, and in the adaxial cuticles the 2920 and 2850 cm^{-1} aliphatic peaks as well, which decline in height with increasing CO_2. However, the change in the height of the 1460 cm^{-1} peak is less obvious in the <1800 cm^{-1} spectra (Fig. S2), so this may be an artefact of the baseline correction in the <3100 cm^{-1} spectra.

Discussion and conclusions

Our results suggest that, at least in terms of broad scale chemical signals, changes in atmospheric CO_2 concentrations only have a limited impact upon *Ginkgo* cuticle chemistry. While this is not an encouraging outcome for developing new CO_2 proxies from FTIR analysis of cuticles, it does suggest that any taxonomic signature present in fossil cuticles will be robust to the ambient CO_2 concentration that the plant was growing in. Chemotaxonomic approaches should therefore be applicable across varying CO_2 regimes. There is some evidence for a decrease in the aliphatic peaks, which may relate to decreases in the epicuticular or intracuticular waxes with increasing CO_2, although these are most obvious with the adaxial spectra where the quantity of data is limited. A more obvious driver of differences in chemistry was the difference between abaxial and adaxial cuticles, related to differences in the cutin matrix and intracuticular phenolic compounds. These findings require investigation with a larger dataset, incorporating more taxa and increased replication of both abaxial and adaxial surfaces.

It will also be necessary to confirm the generality of these results using processed and isolated cuticles where non-fossilisable components have been removed (e.g. Mösle et al. 1998). This will allow for a better comparison with fossil material, including building chemical libraries of modern taxa that can be used to classify fossil specimens. However, the recognition of peaks from previous studies of chemically and mechanically isolated cuticles (e.g. Heredia-Guerrero et al. 2014) in our IR spectra demonstrates that working with the outer surfaces of intact leaves can provide generally applicable information on the drivers of cuticle chemical variability. ATR analysis of unprocessed leaf surfaces provides a rapid means of

253 assessing cuticle chemistry, with field measurements a possibility if a handheld ATR is used
254 (Ribeiro da Luz 2006).
255
256 Our small-scale study does not rule out a possible influence of CO_2 on cuticle
257 chemistry, but it does suggest that the effects are likely to be subtle. In addition to increasing
258 the number of taxa, plants and leaves analysed, spectral deconvolution and curve fitting
259 approaches (e.g. Zodrow and Mastalerz 2001; Depciuch et al. 2018) may help to reveal small
260 differences across CO_2 treatments that might not be detected with the broad scale methods
261 used here. In particular, changes in the carbon isotope composition of the cuticle with
262 increasing CO_2 concentrations may cause small shifts in IR peak positions (Esler et al. 2000),
263 which if consistent across individuals and taxa may be detectable with careful analysis.
264
265 In addition to CO_2, other possible influencing factors will need to be tested for before
266 cuticle chemistry can be confidently used as a taxonomic tool across palaeoenvironments and
267 time periods. Of critical importance will be determining how well chemical signals from
268 external environmental conditions preserve in fossil cuticles. As already noted, one likely
269 driver of cuticle chemical change will be variations in UV-B irradiance, which are known to
270 control concentrations of UV-B absorbing compounds (UACs) in plant tissues (Rozema et al.
271 1999; Neitzke and Therburg 2003; Gonzalez et al. 2007; Rozema et al. 2009). The
272 concentration of UACs in pollen and spore walls has been shown to covary with ambient
273 UV-B flux, and this relationship has been consistently demonstrated across a range of taxa
274 and time periods (Rozema et al. 1999; Rozema et al. 2001a; Rozema et al. 2001b; Blokker et
275 al. 2005; Blokker et al. 2006; Watson et al. 2007; Lomax et al. 2008; Rozema et al. 2009;
276 Fraser et al. 2011; Willis et al. 2011; Lomax et al. 2012; Fraser et al. 2014; Lomax and Fraser
277 2015; Jardine et al. 2016; Jardine et al. 2017). As in pollen and spores, phenolic compounds

take on the role of UACs in cuticles, and these have shown to be preserved in Paleocene *Ginkgo* cuticle (Blokker et al. 2006). Aromatic peaks are also present in FTIR spectra from a range of fossil taxa analysed by Vajda et al. (2017), including specimens dating from the latest Triassic. The relative importance of UV-B flux and taxonomy/phylogeny for controlling cuticle chemistry will therefore need to be investigated, but there is scope for cuticle chemistry to be developed as a palaeo-UV-B proxy, as has been the case with pollen and spores (Blokker et al. 2006; de Leeuw et al. 2006; Rozema et al. 2009).

Acknowledgements

We thank Benjamin Bomfleur, Michael Krings and Christian Pott for the invitation to contribute to this special issue of *PalZ*, and Hans Kerp for his many years of research into the interpretation and use of cuticlar remains. We also thank Vivi Vajda and one anonymous reviewer for their reviews, and Benjamin Bomfleur and Mike Reich for editorial comments. This research was supported by the Palaeontological Association (PEJ: PA-RG201802) and the Natural Environment Research Council (BHL, WTF, MK: NE/R001324/1; WTF: NE/P013724/1).

References

Abu Hamad, A., P. Blomenkemper, H. Kerp, and B. Bomfleur. 2017. *Dicroidium bandelii* sp. nov. (corystospermalean foliage) from the Permian of Jordan. *Paläontologische Zeitschrift* 91: 641–648. doi:10.1007/s12542-017-0384-2.

Abu Hamad, A., H. Kerp, B. Vörding, and K. Bandel. 2008. A Late Permian flora with *Dicroidium* from the Dead Sea region, Jordan. *Review of Palaeobotany and Palynology* 149: 85–130.

Blokker, P., P. Boelen, R. Broekman, and J. Rozema. 2006. The occurrence of *p*-coumaric acid and ferulic acid in fossil plant materials and their use as UV-proxy. *Plant Ecology* 182: 197–207.

Blokker, P., D. Yeloff, P. Boelen, R.A. Broekman, and J. Rozema. 2005. Development of a Proxy for Past Surface UV-B Irradiation: A Thermally Assisted Hydrolysis and Methylation py-GC/MS Method for the Analysis of Pollen and Spores. *Analytical Chemistry* 77: 6026–6031.

Bomfleur, B., A.L. Decombeix, I.H. Escapa, A.B. Schwendemann, and B. Axsmith. 2013. Whole-plant concept and environment reconstruction of a *Telemachus* conifer (Voltziales) from the Triassic of Antarctica. *International Journal of Plant Sciences* 174 (3): 425–444. doi:10.1086/668686.

Collinson, M.E., P. Finch, B. Mösle, R. Wilson, and A.C. Scott. 1999. Preservation of plant cuticles. *Acta Palaeobotanica* Supplement 2: 629–632.

D'Angelo, J.A. 2006. Analysis by Fourier transform infrared spectroscopy of *Johnstonia* (Corystospermales, Corystospermaceae) cuticles and compressions from the Triassic of Cacheuta, Mendoza, Argentina. *Ameghiniana* 43 (4): 669–685.

D'Angelo, J.A., L.B. Escudero, W. Volkheimer, and E.L. Zodrow. 2011. Chemometric analysis of functional groups in fossil remains of the *Dicroidium* flora (Cacheuta, Mendoza, Argentina): Implications for kerogen formation. *International Journal of Coal Geology* 87: 97–111. doi:10.1016/j.coal.2011.05.005.

D'Angelo, J.A., and E.L. Zodrow. 2015. Chemometric study of structural groups in medullosalean foliage (Carboniferous, fossil Lagerstätte, Canada): Chemotaxonomic implications. *International Journal of Coal Geology* 138: 42–54. doi:10.1016/j.coal.2014.12.003.

D’Angelo, J.A., E.L. Zodrow, and A. Camargo. 2010. Chemometric study of functional groups in Pennsylvanian gymnosperm plant organs (Sydney Coalfield, Canada): Implications for chemotaxonomy and assessment of kerogen formation. *Organic Geochemistry* 41: 1312–1325. doi:10.1016/j.orggeochem.2010.09.010.

Dell'Anna, R., P. Lazzeri, M. Frisanco, F. Monti, F. Malvezzi Campeggi, E. Gottardini, and M. Bersani. 2009. Pollen discrimination and classification by Fourier transform infrared (FT-IR) microspectroscopy and machine learning. *Analytical and bioanalytical chemistry* 394 (5): 1443–1452. doi:10.1007/s00216-009-2794-9.

Depciuch, J., I. Kasprzyk, E. Drzymała, and M. Parlinska-Wojtan. 2018. Identification of birch pollen species using FTIR spectroscopy. *Aerobiologia* 34: 525–538. doi:10.1007/s10453-018-9528-4.

Diefendorf, A. F., K. E. Mueller, S. L. Wing, P. L. Koch, and K. H. Freeman. 2010. Global patterns in leaf 13C discrimination and implications for studies of past and future climate. *Proceedings of the National Academy of Sciences USA* 107 (13): 5738–5743. doi:10.1073/pnas.0910513107.

Dominguez, E., M. D. Fernandez, J. C. Hernandez, J. P. Parra, L. Espana, A. Heredia, and J. Cuartero. 2012. Tomato fruit continues growing while ripening, affecting cuticle properties and cracking. *Physiologia Plantarum* 146 (4): 473–486. doi:10.1111/j.1399-3054.2012.01647.x.

Dominguez, E., J. A. Heredia-Guerrero, and A. Heredia. 2017. The plant cuticle: old challenges, new perspectives. *Journal of Experimental Botany* 68 (19): 5251–5255. doi:10.1093/jxb/erx389.

Domínguez, E., J.A. Heredia-Guerrero, and A. Heredia. 2011. The biophysical design of plant cuticles: an overview. *New Phytologist* 189: 938–949. doi:10.1111/j.1469-8137.2010.03553.x.

Esler, M.B., D.W.T. Griffith, S.R. Wilson, and L.P. Steele. 2000. Precision Trace Gas Analysis by FT-IR Spectroscopy. 2. The $^{13}C/^{12}C$ Isotope Ratio of CO_2. *Analytical Chemistry* 72: 216–221.

Foster, G.L., D.L. Royer, and D.J. Lunt. 2017. Future climate forcing potentially without precedent in the last 420 million years. *Nature Communications* 8 (14845). doi:10.1038/ncomms14845.

Fraser, W.T., B.H. Lomax, P.E. Jardine, W.D. Gosling, and M.A. Sephton. 2014. Pollen and spores as a passive monitor of ultraviolet radiation. *Frontiers in Ecology and Evolution* 2. doi:10.3389/fevo.2014.00012.

Fraser, W.T., M.A. Sephton, J.S. Watson, S. Self, B.H. Lomax, D.I. James, C.H. Wellman, T.V. Callaghan, and D.J. Beerling. 2011. UV-B absorbing pigments in spores: biochemical responses to shade in a high-latitude birch forest and implications for sporopollenin-based proxies of past environmental change. *Polar Research* 30: 8312. doi:10.3402/polar.v30i0.8312.

Gill, F. L., J. Hummel, A. R. Sharifi, A. P. Lee, and B. H. Lomax. 2018. Diets of giants: the nutritional value of sauropod diet during the Mesozoic. *Palaeontology* 61 (5): 647–658. doi:10.1111/pala.12385.

Gonzalez, J. A., M. G. Gallardo, C. Boero, M.L. Cruz, and F. E. Prado. 2007. Altitudinal and seasonal variation of protective and photosynthetic pigments in leaves of the world's highest elevation trees *Polylepis tarapacana* (Rosaceae). *Acta Oecologica* 32: 36–41.

Gupta, N.S. 2014. *Biopolymers: a molecular paleontology approach*. Topics in Geobiology, vol. 38. Dordrecht: Springer.

Gupta, N.S., D.E.G. Briggs, M.E. Collinson, R.P. Evershed, R. Michels, K.S. Jack, and R.D. Pancost. 2007a. Evidence for the in situ polymerisation of labile aliphatic organic compounds during the preservation of fossil leaves: Implications for organic matter

376 preservation. *Organic Geochemistry* 38: 499–522.
377 doi:10.1016/j.orggeochem.2006.06.011.
378 Gupta, N.S., R. Michels, D.E.G. Briggs, M.E. Collinson, R.P. Evershed, and R.D. Pancost.
379 2007b. Experimental evidence for the formation of geomacromolecules from plant
380 leaf lipids. *Organic Geochemistry* 38 (1): 28–36.
381 doi:10.1016/j.orggeochem.2006.09.014.
382 Heredia-Guerrero, J. A., J. J. Benitez, E. Dominguez, I. S. Bayer, R. Cingolani, A.
383 Athanassiou, and A. Heredia. 2014. Infrared and Raman spectroscopic features of
384 plant cuticles: a review. *Frontiers in Plant Sciences* 5: 305.
385 doi:10.3389/fpls.2014.00305.
386 Innes S.N., L.E. Arve, B. Zimmermann, L. Nybakken, T.I. Melby, K.A. Solhaug, J.E. Olsen,
387 and S. Torre. 2019. Elevated air humidity increases UV mediated leaf and DNA
388 damage in pea (*Pisum sativum*) due to reduced flavonoid content and antioxidant
389 power. *Photochemical and Photobiological Sciences* 18 (2): 387–399. doi:
390 10.1039/c8pp00401c.
391 Jardine, P. E., F.A.J. Abernethy, B. H. Lomax, W. D. Gosling, and W. T. Fraser. 2017.
392 Shedding light on sporopollenin chemistry, with reference to UV reconstructions.
393 *Review of Palaeobotany and Palynology* 238 :1–6.
394 doi:10.1016/j.revpalbo.2016.11.014.
395 Jardine, P. E., W. T. Fraser, B. H. Lomax, M. A. Sephton, T. M. Shanahan, C.S. Miller, and
396 W. D. Gosling. 2016. Pollen and spores as biological recorders of past ultraviolet
397 irradiance. *Scientific Reports* 6 (39269): 1–8. doi:10.1038/srep39269.
398 Julier, A.C.M., P.E. Jardine, A.L. Coe, W.D. Gosling, B.H. Lomax, and W.T. Fraser. 2016.
399 Chemotaxonomy as a tool for interpreting the cryptic diversity of Poaceae pollen.
400 *Review of Palaeobotany and Palynology* 235: 140–147.

401 Kerp, H. 1990. The study of fossil gymnosperms by means of cuticular analysis. *Palaios* 5:
402 548–569.
403 Kerp, H., A. Abu Hamad, B. Vörding, and K. Bandel. 2006. Typical Triassic Gondwanan
404 floral elements in the Upper Permian of the paleotropics. *Geology* 34 (4): 265–268.
405 doi:10.1130/G22187.1.
406 Leeuw, J.W. de, G.J.M. Versteegh, and P.F. van Bergen. 2006. Biomacromolecules of algae
407 and plants and their fossil analogues. *Plant Ecology* 182: 209–233.
408 doi:10.1007/s11258-005-9027-x.
409 Liland, K.H., and B-H. Mevik. 2015. baseline: Baseline Correction of Spectra, R package
410 version 1.2-1, available at: https://CRAN.R-project.org/package=baseline.
411 Littlejohn, G.R., J.C. Mansfield, D. Parker, R. Lind, S. Perfect, M. Seymour, N. Smirnoff, J.
412 Love, and J. Moger. 2015. In vivo chemical and structural analysis of plant cuticular
413 waxes using stimulated Raman scattering microscopy. *Plant Physiology* 168 (1): 18–
414 28. doi: 10.1104/pp.15.00119.
415 Liu N., C. Karunakaran, R. Lahlali, T. Warkentin, and R.A. Bueckert. 2019. Genotypic and
416 heat stress effects on leaf cuticles of field pea using ATR-FTIR spectroscopy. *Planta*
417 249 (2): 601–613. doi: 10.1007/s00425-018-3025-4.
418 Lomax, B.H., and W.T. Fraser. 2015. Palaeoproxies: Botanical monitors and recorders of
419 atmospheric change. *Palaeontology* 58 (5): 759–768. doi: 10.1111/pala.12180.
420 Lomax, B.H., J. Hilton, R.M. Bateman, G.R. Upchurch, J.A. Lake, I.J. Leitch, A. Cromwell,
421 and C.A. Knight. 2014. Reconstructing relative genome size of vascular plants
422 through geological time. *New Phytologist* 201 (2): 636–644.
423 Lomax, B.H., W.T. Fraser, G. Harrington, S. Blackmore, M.A. Sephton, and N.B.W. Harris.
424 2012. A novel palaeoaltimetry proxy based on spore and pollen wall chemistry. *Earth*
425 *and Planetary Science Letters* 353-354: 22–28. doi:10.1016/j.epsl.2012.07.039.

426 Lomax, B.H., W.T. Fraser, M.A. Sephton, T.V. Callaghan, S. Self, M. Harfoot, J.A. Pyle,
427 C.H. Wellman, and D.J. Beerling. 2008. Plant spore walls as a record of long-term
428 changes in ultraviolet-B radiation. *Nature Geoscience* 1 (9): 592–596.
429 doi:10.1038/ngeo278.
430 Lyons, P.L., W.H. Orem, M. Mastalerz, E.L. Zodrow, A. Vieth-Redemann, and R.M. Bustin.
431 1995. ^{13}C NMR, micro-FTIR and fluorescence spectra, and pyrolysis-gas
432 chromatograms of coalified foliage of late Carboniferous medullosan seed ferns,
433 Nova Scotia, Canada: Implications for coalification and chemotaxonomy.
434 *International Journal of Coal Geology* 27: 227–248.
435 McElwain, J. C., and M. Steinthorsdottir. 2017. Paleoecology, Ploidy, Paleoatmospheric
436 Composition, and Developmental Biology: A Review of the Multiple Uses of Fossil
437 Stomata. *Plant Physiology* 174 (2): 650–664. doi:10.1104/pp.17.00204.
438 McElwain, J.C., and W.G. Chaloner. 1995. Stomatal density and index of fossil plants track
439 atmospheric carbon dioxide in the Palaeozoic. *Annals of Botany* 76: 389–395.
440 Mösle, B., M.E. Collinson, P.F. Finch, B.A. Stankiewicz, A.C. Scott, and R. Wilson. 1998.
441 Factors influencing the preservation of plant cuticles: a comparison of morphology
442 and chemical composition of modern and fossil examples. *Organic Geochemistry* 29
443 (5-7): 1369–1380.
444 Mösle, B., M.E. Collinson, A.C. Scott, and P. Finch. 2002. Chemosystematic and
445 microstructural investigations on Carboniferous seed plant cuticles from four North
446 American localities. *Review of Palaeobotany and Palynology* 120: 41–52.
447 Mösle, B., P. Finch, M.E. Collinson, and A.C. Scott. 1997. Comparison of modern and fossil
448 plant cuticles by selective chemical extraction monitored by flash pyrolysis-gas
449 chromatography-mass spectrometry and electron microscopy. *Journal of Analytical*
450 *and Applied Pyrolysis* 40-41: 585–597.

Neitzke, M., and A. Therburg. 2003. Seasonal changes in UV-B absorption in beech leaves (*Fagus sylvatica* L.) along an elevation gradient. *Forstwissenschaftliches Centralblatt* 122: 1–21.

Olcott Marshall, A., and C.P. Marshall. 2014. Vibrational spectroscopy of fossils. *Palaeontology* 58 (5): 201–211. doi:10.1111/pala.12144.

Pappas, C.S., P.A. Tarantilis, P.C. Harizanis, and M.G. Polissiou. 2003. New Method for Pollen Identification by FT-IR Spectroscopy. *Applied Spectroscopy* 57 (1): 23–27.

Peters-Kottig, W., H. Strauss, H. Kerp. 2006. The land plant $\delta^{13}C$ record and plant evolution in the Late Palaeozoic. *Palaeogeography, Palaeoclimatology, Palaeoecology* 240: 237–252.

Ramirez, F.J., P. Luque, A. Heredia, and M.J. Bukovac. 1992. Fourier Transform IR Study of Enzymatically Isolated Tomato Fruit Cuticular Membrane. *Biopolymers* 32: 1425–1429.

R Core Team. 2017. R: A language and environment for statistical computing. Vienna, Austria: R Foundation for Statistical Computing.

Renault, H., A. Alber, N. A. Horst, A. Basilio Lopes, E. A. Fich, L. Kriegshauser, G. Wiedemann et al. 2017. A phenol-enriched cuticle is ancestral to lignin evolution in land plants. *Nature Communications* 8: 14713. doi:10.1038/ncomms14713.

Ribeiro da Luz, B. 2006. Attenuated total reflectance spectroscopy of plant leaves: a tool for ecological and botanical studies. *New Phytologist* 172 (2): 305–318. doi:10.1111/j.1469-8137.2006.01823.x.

Richey, J.D., G.R. Upchurch, I.P. Montañez, B.H. Lomax, M.B. Suarez, N.M.J. Crout, R.M. Joeckele, G.A. Ludvigson, and J.J. Smith. 2018. Changes in CO2 during Ocean Anoxic Event 1d indicate similarities to other carbon cycle perturbations. *Earth and Planetary Science Letters* 491: 172–182.

476 Rozema, J., P. Blokker, M. A. Mayoral Fuertes, and R. Broekman. 2009. UV-B absorbing
477 compounds in present-day and fossil pollen, spores, cuticles, seed coats and wood:
478 evaluation of a proxy for solar UV radiation. *Photochemical & photobiological*
479 *sciences* 8 (9): 1233–1243. doi:10.1039/b904515e.
480 Rozema, J., R.A. Broekman, P. Blokker, B. Meijkamp, N. de Bakker, J. van de Staaij, A. van
481 Beem, F. Ariese, and S.M. Kars. 2001a. UV-B absorbance and UV-B absorbing
482 compounds (*para*-coumaric acid) in pollen and sporopollenin: the perspective to track
483 historic UV-B levels. *Journal of Photochemistry and Photobiology B: Biology* 62:
484 108–117.
485 Rozema, J., A.J. Noordjik, R.A. Broekman, A. van Beem, B.M. Meijkamp, N.V.J. de Bakker,
486 J.W.M. van de Staaij et al. 2001b. (Poly)phenolic compounds in pollen and spores of
487 Antarctic plants as indicators of UV-B: A new proxy for the reconstruction of past
488 solar UV-B? *Plant Ecology* 154: 11–26.
489 Rozema, J., J. van de Staaij, L-O. Björn, and N de Bakker. 1999. Depletion of stratospheric
490 ozone and solar UV-B radiation: Evolution of land plants, UV-screens and functions
491 of polyphenolics. In *Stratospheric ozone depletion: The effects of enhanced UV-B*
492 *radiation on terrestrial ecosystems*, ed. J. Rozema, 1–19. Leiden: Backhuys.
493 Salminen, T. A., D. M. Eklund, V. Joly, K. Blomqvist, D. P. Matton, and J. Edqvist. 2018.
494 Deciphering the Evolution and Development of the Cuticle by Studying Lipid
495 Transfer Proteins in Mosses and Liverworts. *Plants* 7 (1). doi:10.3390/plants7010006.
496 Steemans, P., K. Lepot, C.P. Marshall, A. Le Hérissé, E.J. Javaux. 2010. FTIR
497 characterization of the chemical composition of Silurian miospores (cryptospores and
498 trilete spores) from Gotland, Sweden. *Review of Palaeobotany and Palynology* 162
499 (4): 577–590.

Steinthorsdottir, M., C. Elliott-Kingston, and K.L. Bacon. 2018. Cuticle surfaces of fossil plants as a potential proxy for volcanic SO_2 emissions: observations from the Triassic–Jurassic transition of East Greenland. *Palaeobiodiversity and Palaeoenvironments* 98: 49. doi:10.1007/s12549-017-0297-9.

Steinthorsdottir, M., V. Vajda, and M. Pole. 2018. Significant transient *p*CO2 perturbation at the New Zealand Oligocene-Miocene transition recorded by fossil plant stomata. *Palaeogeography, Palaeoclimatology, Palaeoecology* 515: 152–161.

Stevens, A., and L. Ramirez-Lopez. 2013. An introduction to the prospectr package. R package Vignette, R package version 0.1.3, available at: https://cran.r-project.org/web/packages/prospectr/vignettes/prospectr-intro.pdf.

Tegelaar, E.W., J. Wattendorff, and J.W. de Leeuw. 1993. Possible effects of chemical heterogeneity in higher land plant cuticles on the preservation of its ultrastructure upon fossilization. *Review of Palaeobotany and Palynology* 77: 149–170.

Vajda, V., M. Pucetaite, S. McLoughlin, A. Engdahl, J. Heimdal, and P. Uvdal. 2017. Molecular signatures of fossil leaves provide unexpected new evidence for extinct plant relationships. *Nature Ecology and Evolution* 1 (8): 1093–1099. doi:10.1038/s41559-017-0224-5.

Villena, J.F., E. Domínguez, and A. Heredia. 2000. Monitoring Biopolymers Present in Plant Cuticles by FT-IR Spectroscopy. *Journal of Plant Physiology* 156: 419–422. doi:10.1016/S0176-1617(00)80083-8.

Watson, J.S., M.A. Septhon, S.V. Sephton, S. Self, W.T. Fraser, B.H. Lomax, I. Gilmour, C.H. Wellman, and D.J Beerling. 2007. Rapid determination of spore chemistry using thermochemolysis gas chromatography-mass spectrometry and micro-Fourier transform infrared spectroscopy. *Photochemical and Photobiological Sciences* 6: 689–694. doi:10.1039/b617794h.

525 Willis, K. J., A. Feurdean, H. J. B. Birks, A. E. Bjune, E. Breman, R. Broekman, J. A.
526 Grytnes, M. New, J. S. Singarayer, and J. Rozema. 2011. Quantification of UV-B flux
527 through time using UV-B-absorbing compounds contained in fossil *Pinus*
528 sporopollenin. *New Phytologist* 192 (2): 553–560. doi:10.1111/j.1469-
529 8137.2011.03815.x.
530 Woodward, F.I. . 1987. Stomatal numbers are sensitive to increases in CO_2 from pre-
531 industrial levels. *Nature* 327: 617–618.
532 Zhiyan, Z., and W. Xiangwu. 2006. The rise of ginkgoalean plants in the early Mesozoic: a
533 data analysis. *Geological Journal* 41: 363–375. doi:10.1002/gj.1049.
534 Zimmermann, B., and A. Kohler. 2014. Infrared spectroscopy of pollen identifies plant
535 species and genus as well as environmental conditions. *Plos One* 9 (4): 1–12.
536 doi:10.1371/journal.pone.0095417.t001.
537 Zimmermann, B., V. Tafintseva, M. Bağcıoğlu, M. Høegh Berdahl, and A. Kohler. 2016.
538 Analysis of Allergenic Pollen by FTIR Microspectroscopy. *Analytical Chemistry* 88:
539 803–811. doi:10.1021/acs.analchem.5b03208.
540 Zodrow, E.L., J.A. D'Angelo, R. Helleur, and Z. Simunek. 2012a. Functional groups and
541 common pyrolysate products of *Odontopteris cantabrica* (index fossil for the
542 Cantabrian Substage, Carboniferous). *International Journal of Coal Geology* 100: 40–
543 50. doi:10.1016/j.coal.2012.06.002.
544 Zodrow, E.L., J.A. D'Angelo, M. Mastalerz, and D. Keefe. 2009. Compression–cuticle
545 relationship of seed ferns: Insights from liquid–solid states FTIR (Late Palaeozoic–
546 Early Mesozoic, Canada–Spain–Argentina). *International Journal of Coal Geology*
547 79: 61–73. doi:10.1016/j.coal.2009.06.001.
548 Zodrow, E.L., J.A. D'Angelo, W.A. Taylor, T. Catelani, J. A. Heredia-Guerrero, and M.
549 Mastalerz. 2016. Secretory organs: Implications for lipoid taxonomy and kerogen

formation (seed ferns, Pennsylvanian, Canada). *International Journal of Coal Geology* 167: 184–200. doi:10.1016/j.coal.2016.10.004.

Zodrow, E.L., and M. Mastalerz. 2001. Chemotaxonomy for naturally macerated tree-fern cuticles (Medullosales and Marattiales), Carboniferous Sydney and Mabou Sub-Basins, Nova Scotia, Canada. *International Journal of Coal Geology* 47: 255–275.

Zodrow, E.L., and M. Mastalerz. 2002. FTIR and py-GC-MS spectra of true-fern and seed-fern sphenopterids (Sydney Coalfield, Nova Scotia, Canada, Pennsylvanian). *International Journal of Coal Geology* 51: 111–127.

Zodrow, E.L., and M. Mastalerz. 2009. A proposed origin for fossilized Pennsylvanian plant cuticles by pyrite oxidation (Sydney Coalfield, Nova Scotia, Canada). *Bulletin of Geosciences* 84 (2): 227–240. doi:10.3140/bull.geosci.1094.

Zodrow, E.L., M. Mastalerz, and R. Helleur. 2012b. *Lepidodendron dawsonii*: functional groups and pyrolysates of compression and fossilized-cuticle (Late Asturian, Canada). *Geologica Croatica* 65 (3): 367–374.

Zodrow, E.L., M. Mastalerz, W.H. Orem, Z. Simunek, and A.R. Bashforth. 2000. Functional groups and elemental analyses of cuticular morphotypes of *Cordaites principalis* (Germar) Geinitz, Carboniferous Maritimes Basin, Canada. *International Journal of Coal Geology* 45: 1–19.

570 **Table 1** IR absorbance peaks measured from the *Ginkgo* cuticles, shown in Figs. 5 and S2.

571 Peak heights were measured as the maximum absorbance value within the given

572 measurement range. Peak assignments and cuticle component interpretations are from

573 Heredia-Guerrero et al. (2014). *v* = stretching, *δ* = bending, *a* = asymmetric, *s* = symmetric

Assignment	Peak position (cm^{-1})	Measurement range (cm^{-1})	Cuticle component
$v_a(CH_2)$	2920	2900 - 2940	Cutin, waxes
$v_s(CH_2)$	2850	2830 - 2870	Cutin, waxes
v(C=O) ester	1710	1695 - 1720	Cutin
v(C-C) aromatic	1600	1595 - 1615	Phenolic compounds
v(C-C) aromatic (conjugated with C=C)	1515	1505 - 1525	Phenolic compounds
$\delta(CH_2)$	1460	1450 - 1470	Cutin, waxes
v_a(C-O-C) ester	1167	1155 - 1180	Cutin
v(C-O)	1020	1010 - 1030	Polysaccharides

574

Figures

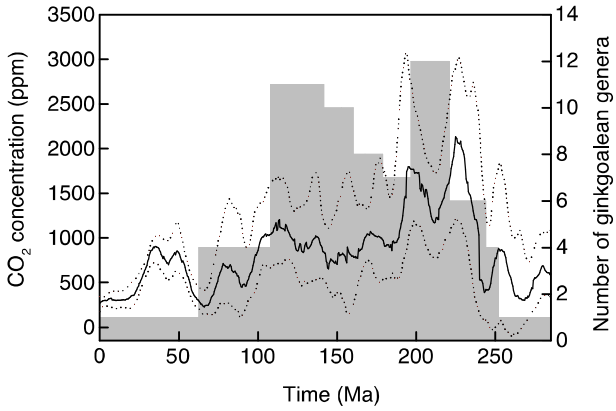

Fig 1 Atmospheric CO_2 (ppm) and changes in ginkgoalean diversity through time. CO_2 data are the Foster et al. (2017) LOESS compilation based on literature data assembled by integrating five independent proxies (stomata, pedogenic $\delta^{13}C$, liverwort $\delta^{13}C$, foraminiferal $\delta^{11}B$ and alkenone $\delta^{13}C$). See SOM of Foster et al. (2017) for full details. Ginkgoalean diversity is taken from Figure 1 of Zhiyan and Xiangwu (2006) and refers to the number of genera/ morphogenera as recorded by the presence of vegetative organs

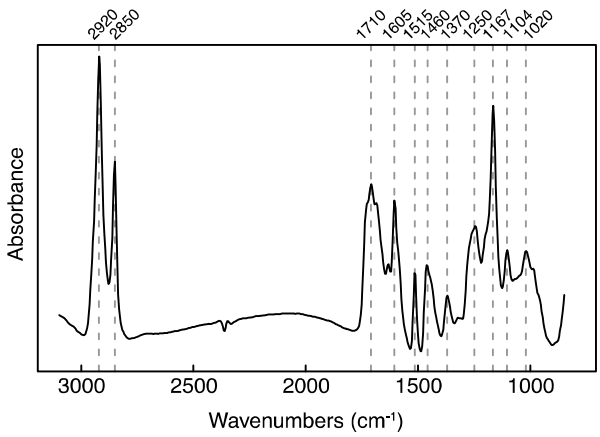

584

585 **Fig 2** Mean ATR-FTIR spectrum for the 400 ppm abaxial (lower leaf surface) cuticles,

586 showing the main peaks mentioned in the text

587

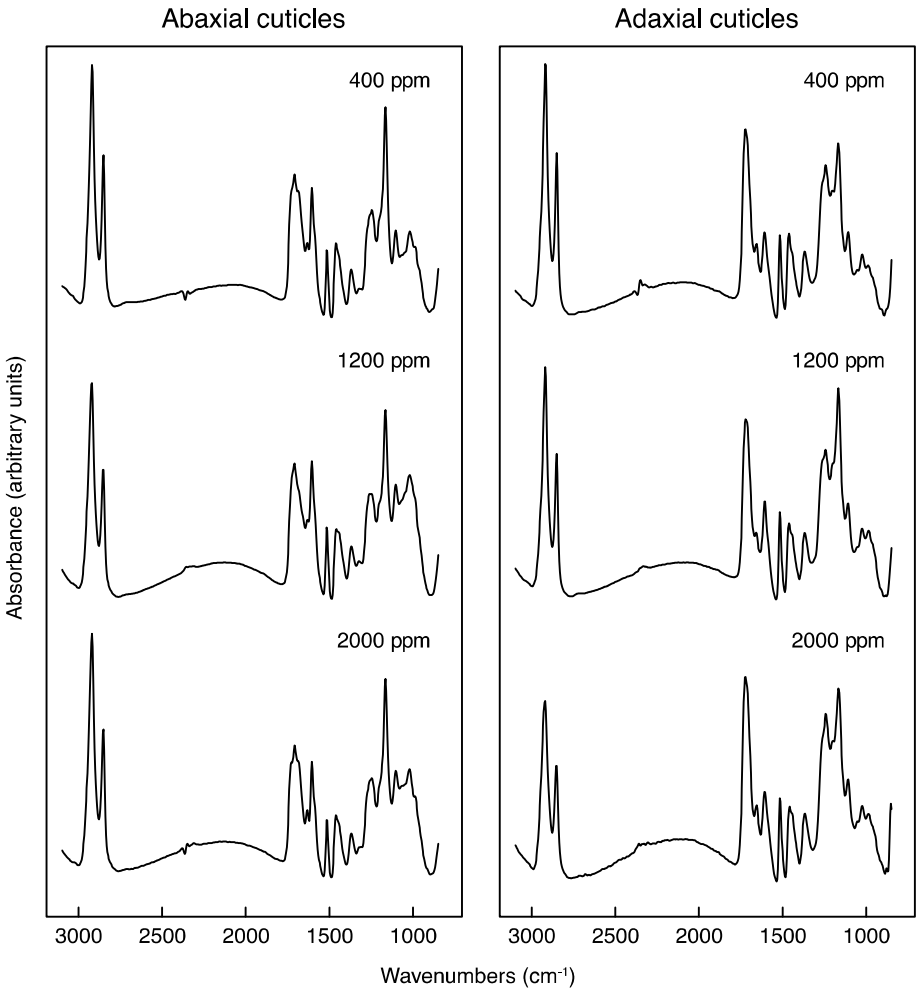

588

589 **Fig 3** Mean ATR-FTIR spectrum for each CO_2 treatment by leaf surface combination.

590 Abaxial = lower leaf surface, adaxial = upper leaf surface

591

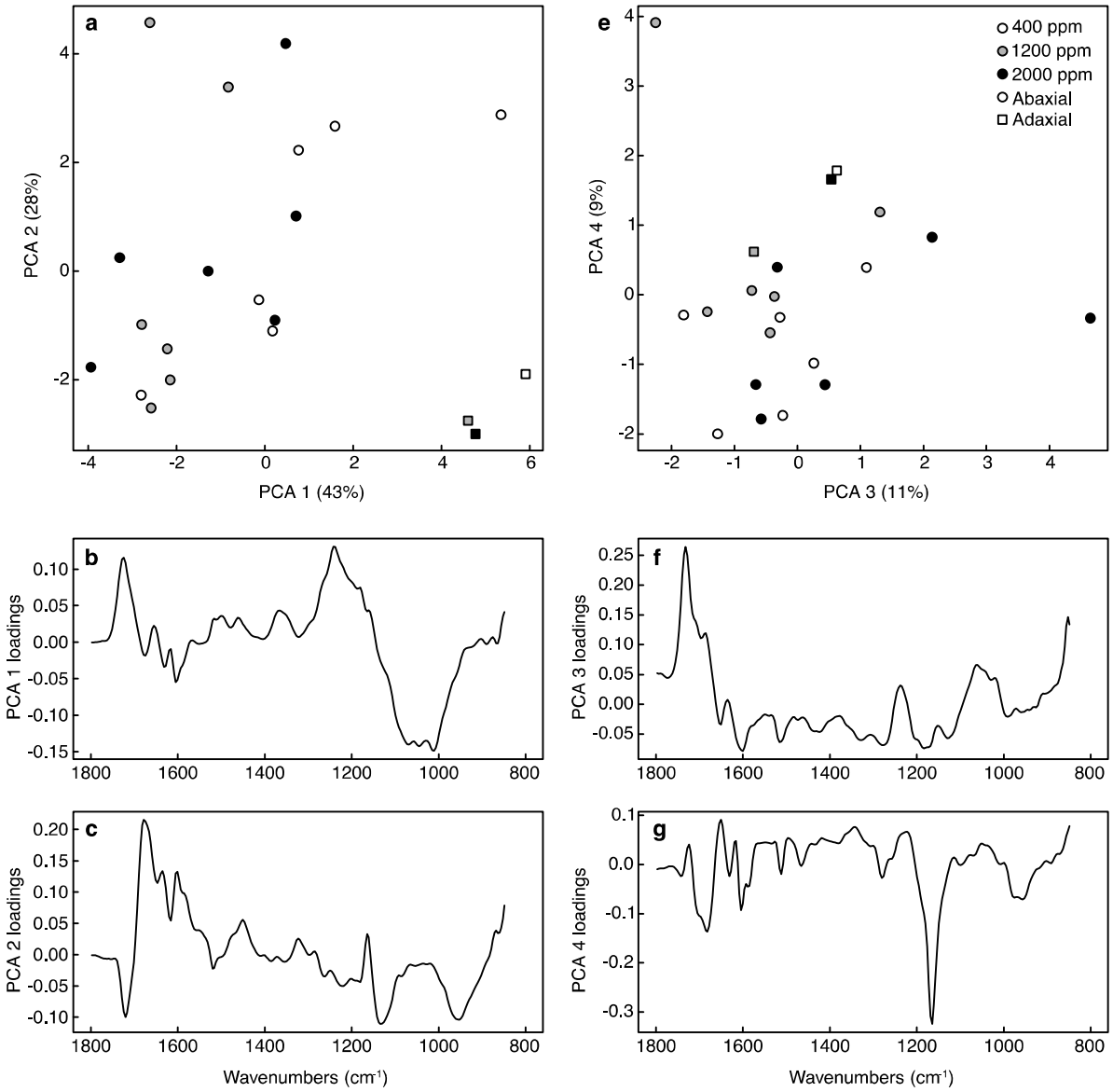

592

593 **Fig 4** Principal Component Analysis (PCA) plots for *Ginkgo* leaf cuticle ATR-FTIR data,

594 with data points representing leaf disc mean spectra. **a** and **e** PCA axes 1 versus 2, and 3

595 versus 4, respectively. Values in parentheses are the percentage of variance in the data

596 explained by each PCA axis. **b**, **c**, **e** and **f** Loadings plots for the PCA axes

597

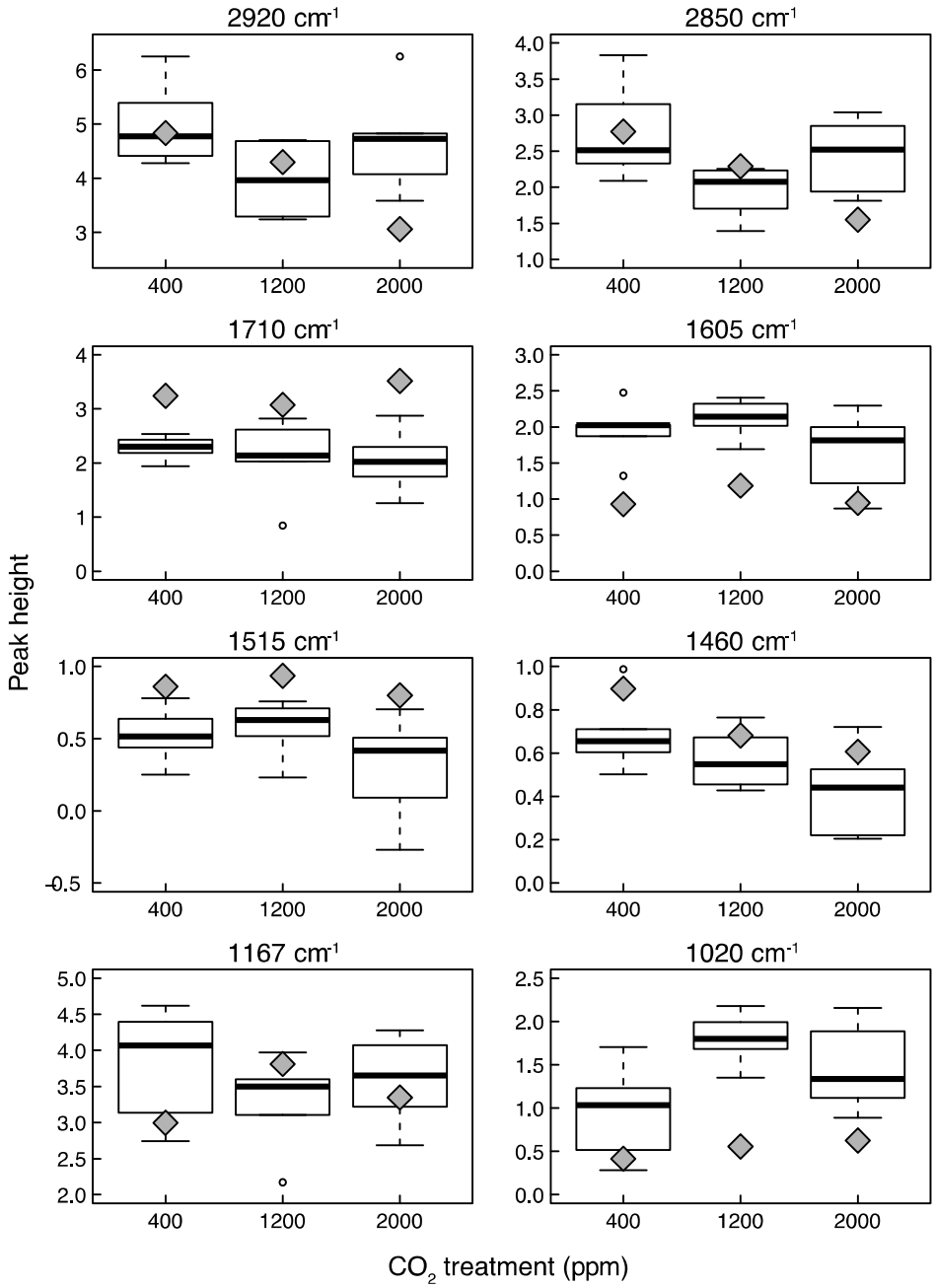

598

599 **Fig 5** Heights of selected IR absorbance peaks grouped by CO_2 treatment, for the <3100 cm^{-1}

600 spectra. Abaxial (lower leaf surface) cuticle data are shown as boxplots, where the thick

601 horizontal line denotes the median value, the edges of the box the upper and lower quartiles,

602 and the whiskers the extremes of the data, up to a limit of 1.5 times the interquartile range

603 (values beyond this are shown as individual circles). Adaxial (upper leaf surface) cuticle data

604 are shown as grey diamonds. See Fig. S2 for peak heights measured from the <1800 cm^{-1}

605 data